2. V. A. Baryshev, "On the influence of random atmosphere inhomogeneities on the intensity of earth's departing thermal radiation," Problems of Physics of the Atmosphere [in Russian], No. 3, Leningrad State Univ. (1963), pp. 105-110.
3. R. M. Kowalik and C. H. Kruger, "The effect of fluctuations and nonuniformities on line-reversal temperature measurements," JQSRT, 18, No. 5, 627-636 (1977).
4. J. W. Dayly, "Effect of turbulence on line-reversal temperature measurements," JQSRT, 17, No. 3, 339-341 (1977).
5. V. P. Kabashnikov and G. I. Kmit, "Influence of turbulent pulsations on thermal radiation," Zh. Prikl. Spektrosk., 31, No. 2, 226-231 (1979).
6. V. P. Kabashnikov and G. I. Kmit, "Taking account of the influence of turbulent pulsations on the thermal radiation of a medium in a square approximation," Inzh.-Fiz. Zh., 37, No. 3, 405-411 (1979).
7. J. S. Draper, L. S. Bernstein, and W. K. Cheng, "Fluctuating emission from molecular vibration—rotational bands," JQSRT, 23, No. 3, 323-326 (1980).
8. P. Gouttenbroze, "On the effect of temperature fluctuations on line intensities," JQSRT, 30, No. 3, 193-211 (1983).
9. Yu. A. Popov, "On the influence of temperature pulsations on flame radiation and the spectrum line-inversion method," Teplofiz. Vys. Temp., 18, No. 2, 383-386 (1980).
10. V. I. Klyatskin, Stochastic Equations and Waves in Randomly Inhomogeneous Media [in Russian], Nauka, Moscow (1980).

NONUNIFORMITY OF THE VELOCITY FIELD OF A FLUX PASSING THROUGH A PACKED BED

M. A. Gol'dshtik, A. M. Vaisman,
A. V. Lebedev, and M. Kh. Pravdina

UDC 532.546.2

It is experimentally and theoretically shown that the sharp nonuniformity of the velocity at the outlet from a packed bed develops outside the bed as the flow passes through a curvilinear boundary.

The strongly pronounced nonlocalized velocity nonuniformity in a flow emerging from a packed bed has been investigated experimentally [1-5] and theoretically [4, 6-8] for a period of more than over 20 years. However, complete clarity with regard to the character and nature of this phenomenon has not yet been achieved. Experiments indicate that the nonuniformity scale is more likely connected with the channel dimensions than with the bead diameter. Theoretical investigations are based on the assumption that the velocity nonuniformity develops within the packed bed due to changes in its porosity, caused by repacking or deformations. For all the diversity of the deformation models used, the interaction between the bed and the channel walls plays the central role. An alternative approach is based on the possibility that the deflection of the supporting grid may be the cause of velocity nonuniformity [5]. This possibility has not been investigated to a sufficient extent. Therefore, we have performed experiments in order to compare the effect of the walls with that of the supporting grid.

The device for blowing air through a bed of beads (Fig. 1a) makes it possible to vary the deflection of the supporting grid and also introduce an additional wall, not connected to the grid, in the middle of the channel (Fig. 1b). The device consists of a vertical, rectangular channel with a 120 × 60 mm cross section, which has three parts: the supply section 5, the operating section 6, and the outlet channel 7. The endfaces of the channel sections have flanges with rubber gaskets providing an airtight seal. Air is supplied to the channel from the main at pressures of up to 8 atm through branch pipe 1 and is then transmitted through swirler 2 and equalizer 3. In spite of its small dimensions, this inlet arrangement ensures relatively good equalization of the air flow ahead of the bead bed

Institute of Thermophysics, Siberian Branch, Academy of Sciences of the USSR, Novosibirsk. Translated from Inzhenerno-Fizicheskii Zhurnal, Vol. 49, No. 1, pp. 42-51, July, 1985. Original article submitted July 4, 1984.

 0022-0841/85/4901-0784$09.50

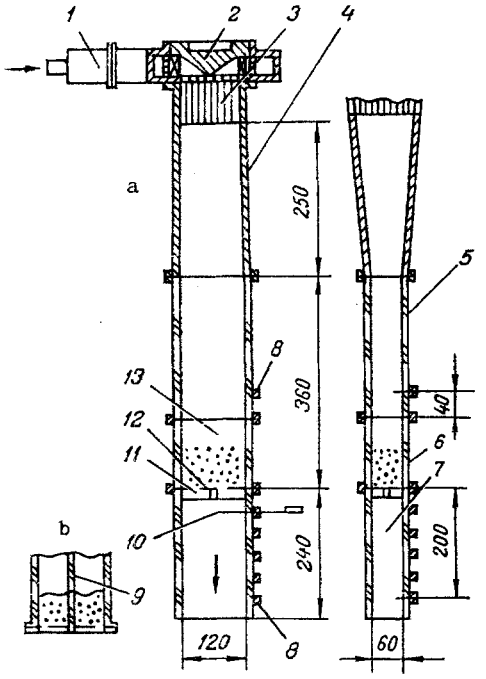

Fig. 1. Schematic of the experimental device.

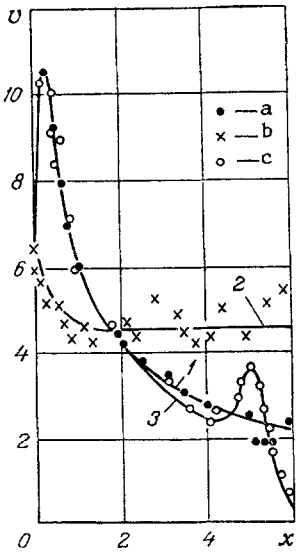

Fig. 2. Velocity profile at outlet from the bed of beads [v (m/sec); x (cm)]. a) Freely sagging grid; b) grid supported by cross brace; c) separating wall provided in the middle of the channel.

13. Connection between the equalizing device and the main channel is provided by section 4, which consists of a tube with a diameter of 114 mm that passes into a rectangular duct with a 120 × 60 mm cross section. Sealing grommets 8 for inserting the hot-wire anemometer sensing element 10 are provided in the walls of the supply and outlet channels. The operating section has fastenings for grids and the dividing wall 9. In order to reduce the deflection of grid 12 under the weight of particles, a support 11 is provided in the form of a cross brace, which is fastened by means of screws in the outlet channel walls and is in direct contact with the load-free lower grid.

The basic experimental results are shown in Fig. 2. Metal beads with the diameter d = 2.6 mm served as the granular material. They were poured onto a stainless-steel grid with 0.65 mm mesh. Curve 1 pertains to the grid with free deflection. It displays the typical pattern of "ears" with the ratio $v_{max}/v_{min} = 5$. When the taut load-free grid was supported from below by the cross brace, which divided the grid into four equal parts, as a result of which the grid deflection was reduced by a factor of 16 for the same load, the flow pattern changed drastically: Curve 2 displayed a local nonuniformity with an extent of about 3d at the wall. The above ratio amounted to $v_{max}/v_{min} = 1.4$. Curve 3 illustrates the effect of a separating wall with a thickness of 18 mm, placed at the middle of the channel. Such a large thickness was necessary for preventing the mutual interference of the flows to the right and to the left of the plate. Measurements were performed at a distance of 10 mm below the grid, where microscopic velocity nonuniformities were smoothed out to a considerable extent. The region of distances from 5.1 to 6 cm corresponds to the wind shadow caused by the insert. It is evident that the flow is virtually unchanged in comparison with the first case over the greater part of the cross section. Local "ears" with $v_{max}/v_{min} = 1.4$ are observed near the separating wall.

These data suggest that the wall presence manifests itself only in slight local velocity nonuniformity, which is related to changes in the packing of beads near the wall. The considerable macroscopic nonuniformities beyond the packed bed are caused by the deflection of the supporting grid. However, this may be accompanied by two factors: First, the deflection promotes deformation of the bed and, second, it alters the geometry of the flow as it emerges from the bed.

Let us separate the first effect. One of the factors causing deformation of the packed bed is the force exerted by the infiltrating flow. The developing deformation, in turn, al-

ters the local porosity and redistributes the flow, which may produce hydrodynamic nonuniformities, which are the greater, the larger the allowable bed deformations. Quantitative data can be obtained by solving simultaneously the hydrodynamic and the deformation equations, which lead to the following problem.

Steady-state filtration through a bed of beads lying on an elastic grid is considered.

The bed resistance α is determined by means of the Kármán–Conseni equation. The filtration problem is stated in the form of the equations

$$\vec{v} = -\frac{1}{\alpha\rho}\operatorname{grad} p, \quad \operatorname{div}\vec{v} = 0, \quad \alpha = \frac{150\nu(1-\varepsilon)^2}{\varepsilon^3 d^2}. \tag{1}$$

Assume that a two-dimensional incompressible flow moves vertically along the y axis through a bed whose thickness is H and half-width is h = 1.

Elimination of the velocity in (1) results in an elliptic equation for p:

$$\frac{\partial}{\partial x}\frac{1}{\alpha}\frac{\partial p}{\partial x} + \frac{\partial}{\partial y}\frac{1}{\alpha}\frac{\partial p}{\partial y} = 0. \tag{2}$$

Strictly speaking, it would have been necessary to state the problem in terms of a combination of filtration flow and free flow (Eq. (2) would then be inadequate by itself), but this would represent a major complication. Therefore, we shall assign approximate conditions at the bed boundaries. Assume that v_y = const = 1 is assigned at the inlet, and p = const at the outlet. Considering the flow symmetry with respect to the x = 0 axis and the impermeability of the walls, we have the following boundary conditions:

$$\left.\frac{\partial p}{\partial y}\right|_{y=0} = -\alpha\rho, \quad p|_{y=H} = 0, \quad \left.\frac{\partial p}{\partial x}\right|_{x=0;\,1} = 0.$$

In order to calculate the stressed state, we use the theory of limiting deformation of a granular medium [7], the equations for which are written in the following form:

$$\frac{\partial p_g}{\partial x_i} + 2\mu\frac{\partial p_g}{\partial x_j}\gamma_{ij} + F_i = 0, \quad \gamma_{ij} = \frac{1}{2}\left(\frac{\partial u_i}{\partial x_j} + \frac{\partial u_j}{\partial x_i}\right), \quad \frac{\partial u_i}{\partial x_i} = 0, \tag{3}$$

where u_i is the displacement vector, p_g is the pressure within the granular medium, $F_i = \partial p/\partial x_i$ are the components of the mass force vector, and μ is a constant, which has the order of unity. The relationship between the porosity ε of the bed and the shearing strain in it is provided by the expression

$$\varepsilon = (\varepsilon_0 + 2\mu\gamma^2)/(1 + 2\mu\gamma^2) \approx \varepsilon_0 + 2\mu(1-\varepsilon_0)\gamma^2, \quad \gamma^2 = \frac{1}{2}\gamma_{ij}\gamma_{ij}. \tag{4}$$

The value of ε_0 represents the initial porosity distribution in the absence of shear.

Expressions (1)–(3) constitute a closed system of equations. By using the notation $\mu\gamma_{ij} \to \gamma_{ij}$ and $\mu u_i \to u_i$, we find from (3)

$$-\frac{\partial p_g}{\partial x} + 2\frac{\partial p_g}{\partial y}\gamma_{xy} + 2\frac{\partial p_g}{\partial x}\gamma_{xx} + p_g\Delta u_x + F_x = 0,$$

$$-\frac{\partial p_g}{\partial y} + 2\frac{\partial p_g}{\partial x}\gamma_{xy} + 2\frac{\partial p_g}{\partial y}\gamma_{yy} + p_g\Delta u_y + F_y = 0.$$

Subsequent transformations are carried out with an accuracy to second-order small quantities with respect to γ with an allowance for the fact that, for γ = 0 and ε_0 = const, $\partial p_g/\partial x = 0$ and $\partial p_g/\partial y$ = const. We have

$$-\frac{\partial p_g}{\partial x} + 2\frac{\partial p_g}{\partial y}\gamma_{xy} + p_g\Delta u_x + F_x = 0,$$

$$-\frac{\partial p_g}{\partial y} + 2\frac{\partial p_g}{\partial y}\gamma_{yy} + p_g\Delta u_y + F_y = 0. \tag{5}$$

Applying the rot (curl) operation to (5), we eliminate the force F:

$$\frac{\partial p_g}{\partial y}\Delta u_x - 2\frac{\partial p_g}{\partial y}\left(\frac{\partial\gamma_{yy}}{\partial x} - \frac{\partial\gamma_{xy}}{\partial y}\right) + p_g\Delta\left(\frac{\partial u_x}{\partial y} - \frac{\partial u_y}{\partial x}\right) = 0.$$

We introduce new variables — the stream function ψ and the vorticity ω — in accordance with the relationships $u_x = \partial\psi/\partial y$, $u_y = -\partial\psi/\partial x$, and $\omega = \partial u_y/\partial x - \partial u_x/\partial y$;

$$\gamma_{yy} = -\frac{\partial^2\psi}{\partial x\partial y}, \quad \gamma_{xy} = \frac{1}{2}\left(\frac{\partial^2\psi}{\partial y^2} - \frac{\partial^2\psi}{\partial x^2}\right),$$

$$\Delta u_x = \frac{\partial^3\psi}{\partial y^3} + \frac{\partial^3\psi}{\partial x^2\partial y} = -\frac{\partial\omega}{\partial y},$$

$$2\left(\frac{\partial\gamma_{yy}}{\partial x} - \frac{\partial\gamma_{xy}}{\partial y}\right) = -2\frac{\partial^3\psi}{\partial x^2\partial y} + \frac{\partial^3\psi}{\partial x^2\partial y} - \frac{\partial^3\psi}{\partial y^3} = -\frac{\partial\Delta\psi}{\partial y} = \frac{\partial\omega}{\partial y}.$$

With these transformations, we obtain the elliptic system

$$\Delta\psi = -\omega, \quad 2\frac{\partial p_g}{\partial y}\frac{\partial\omega}{\partial y} + p_g\Delta\omega = 0, \tag{6}$$

which must be supplemented with the pressure equation, using, for instance, the second equation in (5).

We shall consider the boundary conditions separately for each boundary. The y = 0 boundary is free, so that $p_3 = 0$ at this boundary. We thereby obtain the Cauchy problem for pressure. For y = 0, we obtain the following from the first equation in (5):

$$-\frac{\partial p_g}{\partial y}\left(\frac{\partial^2\psi}{\partial x^2} - \frac{\partial^2\psi}{\partial y^2}\right) + F_x = 0$$

or

$$\frac{\partial^2\psi}{\partial x^2} = -\frac{1}{2}\left(\omega - \frac{\partial p_g/\partial x}{\partial p_g/\partial y}\right). \tag{7}$$

According to the second equation in (6),

$$\partial\omega/\partial y = 0 \quad \text{for} \quad y = 0. \tag{8}$$

The following conditions are imposed at the symmetry axis x = 0:

$$\omega = 0, \quad \psi = 0. \tag{9}$$

We impose the condition for the absence of transverse displacements at the boundary y = H;

$$\partial\psi/\partial y = 0. \tag{10}$$

The equation for a sagging grid is written in the following form [9]:

$$aT_{yy} = \frac{\partial^2 u_y}{\partial x^2}, \tag{11}$$

where $T_{yy} = -p_g + 2p_g\gamma_{yy} = -p_g - 2p_g\frac{\partial^2\psi}{\partial x\partial y} = -p_g$ in view of condition (10). Since $u_y = -\partial\psi/\partial x$, we find from (11)

$$-\frac{\partial^3\psi}{\partial x^3} = ap_g, \quad \frac{\partial^2\psi}{\partial x^2} = a\int_0^x p_g dx$$

or

$$\omega = -\frac{\partial^2\psi}{\partial y^2} - a\int_0^x p_g dx. \tag{12}$$

The coefficient a is connected with the elasticity of the grid. In particular, if $a = 0$, the grid can be considered as absolutely rigid, and the boundary condition (12) signifies impermeability of the boundary, since it follows from this condition that $\partial^2\psi/\partial x^2 = 0$ and $u_y = \text{const}$.

Consider the conditions at the wall, x = 1. It follows from the wall impermeability requirement that

$$\psi = 0. \tag{13}$$

Moreover, if we seek a continuous solution, we must consider that conditions (7), (10), and (12) have already been imposed at the ends of this boundary. The equation $\partial^2\psi/\partial x^2 = -\omega$ follows from (13); on the other hand, since $\partial p/\partial x = 0$ for x = 1, it follows from (7) that $\partial^2\psi/\partial x^2 = -\omega/2$, so that $\omega(1, 0) = 0$. Furthermore, in accordance with (10) and (12),

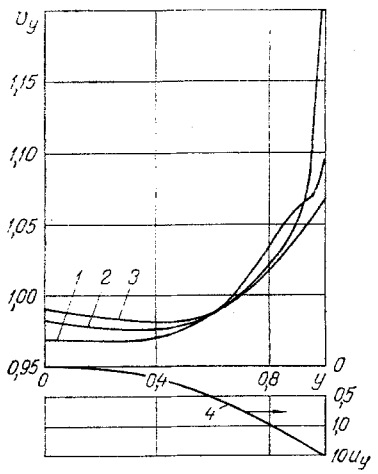

Fig. 3

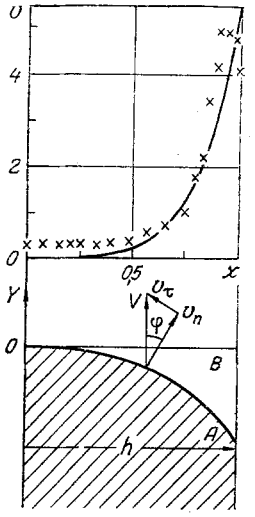

Fig. 4

Fig. 3. Calculation results. 1), 2), and 3) Velocity profiles in the deformed bed corresponding to 1/2, 1/4, and 1/6 sections; 4) shape of the deformed grid.

Fig. 4. Flow through an undeformable porous insert with a curvilinear boundary; approximate calculations and experimental data.

$$\frac{\partial \psi}{\partial y}(1,\ H) = 0, \quad \omega(1,\ H) = -a\int_0^1 p_g\, dx. \tag{14}$$

If we now impose the sticking or slippage conditions at the boundary, the problem becomes overdetermined. This means that it is necessary either to relinquish the conditions for the continuity of the solution of (14) or take into account the interaction between the bed and the wall and determine the sticking and slippage regions by analyzing the friction forces. However, since this interaction cannot take place at a point sufficiently remote from the wall, and we are interested mostly in macroscopic nonuniformities, we shall satisfy requirements (14) by using the condition

$$\omega = -\left(a\int_0^1 p_g dx\right)\left(\frac{y}{H}\right)^2. \tag{15}$$

In the case of a rigid grid, $a = 0$, so that, according to (15),

$$\omega = 0. \tag{16}$$

Condition (16) corresponds to the slippage condition $\gamma_{xy} = 0$.

This nonlinear problem was solved by using the iteration method. At the first stage, the hydrodynamic problem was solved for the known porosity of the bed. We then calculated the resistance forces, solved the deformation problem, and calculated the new nonuniformity.

The process was then repeated until convergence was achieved. All the elliptic equations were solved by using the method of longitudinal and transverse trial runs [9]. A three-dimensional 10 × 20 grid was used. The longitudinal dimension amounted to one-fourth of the channel width.

In investigating the effect of the grid's deflection on bed deformation, the initial porosity distribution was assumed to be uniform: $\varepsilon_0 = 0.37$. The grid deflection was varied by changing the a parameter. Figure 3 shows the velocity profiles $v_y(x)$ in several bed sections for the deflection $\Delta = 0.15$ and the shape of the deformed grid. Table 1 provides data from three calculation variants for different grid deflections. The thus produced velocity nonuniformity is undoubtedly macroscopic, but the effect is weak. A more or less significant value of the v_y^{max}/v_y^{min} ratio corresponds to the huge deflection $\Delta = 0.21$.

TABLE 1. Calculation Results for a Flow Interacting with a Deformable Granular Medium

Grid deflection Δ	$v_y^{max} / \int_0^1 v_y dx$	v_y^{max}/v_y^{min}	ε_{max}
0.15	1,25	1,29	0,40
0,18	1,33	1,38	0,41
0,21	1,44	1,54	0,43

In connection with this, it is of interest to examine the second effect, which is a purely geometric one and is connected with emergence of the flow from the bed through a curvilinear boundary. Assume that the flow in a channel whose width is 2h emerges from a porous medium whose shape is shown in the lower part of Fig. 4, where OY is the symmetry axis. Assume that the OA boundary is, for instance, a parabola,

$$y = -\lambda x^2. \tag{17}$$

At the point A, the flow is directed along the wall, so that the tangential component of velocity V does not vanish. For the tangential and the normal components within the layer, we have

$$v_\tau = V \sin\varphi, \quad v_n = V\cos\varphi,$$

while $\operatorname{tg}\varphi = y' = -2\lambda h$. We shall furthermore use the conditions for joining the flows outside and inside the bed that have been introduced in [10]. According to these conditions, the vorticity

$$\omega = -\frac{\alpha}{\varepsilon}\frac{v_\tau}{v_n} = -\frac{\alpha}{\varepsilon}\operatorname{tg}\varphi = -\alpha y'/\varepsilon \tag{18}$$

arises at the point A. It is difficult to solve the problem on the basis of the exact statement; this can be done only numerically. Therefore, considering that the grid deflection AB = Δ is small ($\Delta/h \ll 1$), let us assume that the outlet flow is parallel to the y axis over the entire section OA. This assumption is certainly wrong. Actually, a singularity must arise at the point A, since, on the one hand, the flow must change direction as it encounters the interface at an angle different from zero, and, on the other hand, its direction at the wall is assigned. At other points of the boundary, the tendency of the flow would be to develop along the normal to OA, following the path of least resistance. However, all these local nonuniformities are smoothed out exponentially downstream, so that, for $y \to \infty$, only vortex nonuniformities remain in the flow. Therefore, we take into account the boundary curvature only in calculating the vorticity while the other conjugation conditions are satisfied by assuming that the boundary is flat. In other words, we assume that relationship (18) holds not only at the point A, but also everywhere on OA, so that

$$\omega = 2\alpha\lambda x/\varepsilon. \tag{19}$$

Moreover, the liquid velocity is to be considered constant and equal to V everywhere in the bed, including the OA surface. Thus, we contemplate the case where nonuniformity arises only beyond the bed as a result of vortex formation at the curvilinear boundary.

Two-dimensional vortex flow of an ideal liquid conforms to the equations [11]

$$\Delta\Psi = -\omega, \quad v_x = \partial\Psi/\partial y, \quad v_y = -\partial\Psi/\partial x, \quad \omega = \omega(\Psi). \tag{20}$$

The function $\omega = \omega(\Psi)$ is found from the boundary conditions at inlet sections, in this case, at OA. According to (20), we have $\Psi = -\varepsilon V x$ with an allowance for the flow symmetry with respect to the y axis. Then, we find from (19) that $\omega = -2\alpha\lambda\Psi/(\varepsilon^2 V)$, and the first equation in (20) assumes the following form:

$$\frac{\partial^2\Psi}{\partial x^2} + \frac{\partial^2\Psi}{\partial y^2} = k^2\Psi. \tag{21}$$

All the variables are given here in dimensionless form; the half-width of the channel h is used as the length scale, and the mean velocity beyond the bed εV is used as the velocity scale. The value of k, which is the basic parameter of the problem, is determined by the relationship

$$k = \frac{h}{\varepsilon}\sqrt{\frac{2\alpha\lambda}{V}}. \tag{22}$$

The sought function Ψ must satisfy the conditions

$$\Psi|_{x=0} = 0, \quad \Psi|_{x=1} = -1, \quad \Psi|_{y=0} = -x. \tag{23}$$

The solution of the problem (21), (23), bounded for $y \to \infty$, is given by

$$\Psi = -\frac{\operatorname{sh} kx}{\operatorname{sh} k} + 2k^2 \sum_{n=1}^{\infty} \frac{(-1)^n}{n\pi(k^2 + n^2\pi^2)} \sin n\pi x \exp\left(y\sqrt{k^2 + n^2\pi^2}\right). \tag{24}$$

Expression (24) makes it possible to estimate the error due to the assumption of a parallel flow in the bed. For this, it is necessary to calculate the value of v_x for y = 0:

$$v_x|_{y=0} = 2k^2 \sum_{n=1}^{\infty} \frac{(-1)^{n+1}}{n\pi(k^2 + n^2\pi^2)} \sin n\pi x. \tag{25}$$

According to (25), $v_x = 0$ for x = 0 and x = 1; the maximum value of v_x occurs for x = 1/2. However, calculations show that, even in this case, the sum in (25) is rather small due to the alternating signs in the series and is a decreasing function of k. Thus, for k = 1, this sum amounts to 0.09. Therefore, for sufficiently small k values, the v_x values are small, and the initial assumption concerning the parallelness of the flow in the bed is justified. With an increase in k, the matching of the tangential velocities at the interface deteriorates, so that we must seek the solution of the conjugate problem, which is very complex due to its nonlinearity. Therefore, with good-quality results in mind, we shall accept solution (24) and consider it as a model solution for large k values, which, in principle, can be realized by choosing the velocity distribution at the inlet to a finite-thickness bed.

The second term in (24) is rapidly damped with respect to y, especially for large k values. However, even for k = 0, the damping is determined by the exponential function $e^{-\pi y}$, which ensures reduction of the sum by a factor of 23 at the half-gauge distance y = 1 from the inlet.

Therefore, for practical purposes, it is sufficient to consider the asymptotic solution, represented by the first term in (24), which reflects the vortex nonuniformities persisting throughout the flow. Thus, we have

$$\Psi = -\operatorname{sh} kx/\operatorname{sh} k. \tag{26}$$

We calculate the velocity $v_y = v$ in accordance with (20):

$$v = k \operatorname{ch} kx/\operatorname{sh} k. \tag{27}$$

The value of v represents the longitudinal flow velocity, reduced to the mean velocity. Therefore, v = 1 for k = 0. The larger the value of k, the more pronounced the flow nonuniformity, while

$$v(1) = k \operatorname{cth} k \to \infty, \quad v(0) = k/\operatorname{sh} k \to 0 \text{ for } k \to \infty.$$

The above relationships characterize this as a nonlocalized nonuniformity, which is also evident from Fig. 4, the upper part of which shows the v(x) profile for k = 5.79. Thus, according to these results, large-scale nonuniformities beyond the packed bed can be explained by purely geometric causes. In order to check this assumption, we carried out a special experiment where, instead of the bead packing, the operating section was filled with an undeformable porous insert with a thickness of 11 mm and a curvilinear boundary in the shape of a parabola, $y = (x - 60)^2/900$, where x and y are given in millimeters. The deflection is equal to $\lambda h^2 = 4$ mm for h = 60 mm. The value of α in experiments was determined with respect to the pressure drop and the discharge; it was found that k = 5.79. The experimental data in dimensionless form are indicated by points in Fig. 4. Control measurements on a similar insert with a flat boundary resulted in a uniform velocity profile. The agreement is evidently fairly good.

Thus, it has been established that even slight geometric factors cause large macroscopic flow nonuniformities beyond the bed; however, they are not hazardous for the equipment.

NOTATION

d, bead diameter; V, v, flow velocity; v_{max} and v_{min}, maximum and minimum velocity values, respectively; v_x, v_y, v_τ, and v_n, horizontal, vertical, tangential, and normal components of the velocity, respectively; x and y, coordinates; ρ, liquid density; ε, bed porosity; ν, viscosity; p, hydrodynamic pressure; α, resistance coefficient; p_g, pressure in the deformable granular medium; μ, constant; u_i, displacements; γ_{ij}, deformation; Ψ, ψ, stream function; ω, vorticity; H, bed height; h, half width of bed; λ and k, parameters.

LITERATURE CITED

1. C. E. Schwartz and J. M. Smith, "Flow distribution in packed beds," Ind. Eng. Chem., 45, No. 6, 1209-1218 (1953).
2. K. Sato and T. Akehata, "Flow distribution in packed beds," Chem. Eng., Jpn., 22, No. 7, 430-436 (1958).
3. E. K. Popov, E. V. Smirnova, G. M. Abaev, et al., "Problems in investigating reaction vessels with fixed catlyst beds," in: Aerodynamics of Chemical Reaction Vessels [in Russian], Institute of Catalysis, Siberian Branch, Academy of Sciences of the USSR, Novosibirsk (1976), pp. 65-71.
4. M. A. Gol'dshtik, A. V. Lebedev, and V. N. Sorokin, "Valve effect in a packed bed," Inzh.-Fiz. Zh., 34, No. 3, 389-393 (1978).
5. V. A. Kirillov, V. A. Kuz'min, V. I. P'yanov, and V. M. Kanaev, "Velocity profile in a fixed packed bed," Dokl. Akad. Nauk SSSR, 245, No. 1, 159-162 (1979).
6. S. S. Grigoryan and Dao Min' Ngok, Hydrodynamic Problems of Chemical Technology [in Russian], Scientific-Research Institute of Mechanics, Moscow State Univ. (1979).
7. A. M. Vaisman and M. A. Gol'dshtik, "Deformation of granular media," Dokl. Akad. Nauk SSSR, 252, No. 1, 61-64 (1980).
8. V. D. Kotelkin and V. P. Myasnikov, "Effect of packing deformation on gas flow in a chemical reaction vessel with a fixed catalyst bed," Dokl. Akad. Nauk SSSR, 247, No. 1, 170-173 (1979).
9. G. I. Marchuk, Methods of Numerical Mathematics, Springer-Verlag (1975).
10. A. M. Vaisman and M. A. Gol'dshtik, "Dynamic model of liquid flow in a porous medium," Izv. Akad. Nauk SSSR, Mekh. Zhidk. Gaza, No. 6, 89-95 (1978).
11. M. A. Gol'dshtik, Vortex Flow [in Russian], Nauka, Novosibirsk (1981).

MODEL FOR CALCULATING THE ROTATIONAL FLOW PARAMETERS OF A TWO-PHASE MEDIUM WITH ALLOWANCE FOR PHASE INTERACTION

É. F. Shurgal'skii

UDC 532.5:533.6.011

A method is proposed for solving the problem of the rotational flow parameters of a two-phase dusty-gas medium in a cylindrical channel. The effect of the solid particles on the carrier flow is demonstrated numerically.

Apparatus using the cyclone effect make it possible to intensify considerably and qualitatively imporve such processes as heat and mass transfer, separation, mixing, and dust collecting. In order to design this apparatus and calculate the operating regimes it is necessary to have data on the hydrodynamic flow parameters of the two-phase medium.

In apparatus with swirling flows the centrifugal forces affect not only the distribution of solid-phase concentration over the cross section [1] but also, what is more important, the aerodynamic characteristics of the carrier gas.

Below we consider a mathematical model and methods of solution applicable to apparatus intended for processing dusty gases. As an example we will take a dust catcher with swirling counterflows (Fig. 1).

Moscow Institute of Chemical Machine Building.

Translated from Inzhenerno-Fizicheskii Zhurnal, Vol. 49, No. 1, pp. 51-57, July, 1985. Original article submitted July 4, 1984.

0022-0841/85/4901-0791$09.50